of a stable Kr isotope and the radioisotope Kr^{81}. This dating method is found to be both accurate and best suited for lunar material for the following reasons: (i) the age determination is based on the isotopic composition of one element only and therefore eliminates errors in concentration measurements; (ii) Sr, Y, and Zr, the main target elements for the production of Kr, are strongly enriched in lunar material, making it possible to measure Kr^{81} in samples as small as 0.1 g; (iii) because of both unusual chemical composition and unusual irradiation conditions the production rates of those stable isotopes generally used for age determinations are not well known.

Kr-Kr ages are obtained from the equation (*5*)

$$T_r = \frac{Kr^{83}{}_{spall}}{Kr^{81}} \frac{P_{81}}{P_{83}} \frac{1}{\lambda}$$

where $\lambda = 3.3 \times 10^{-6}$ per year, and $P_{81} = (0.95 \pm 0.05)(P_{80} + P_{82})/2$.

The relative production rates of the Kr isotopes are similar for all the investigated rocks, which is indicated by rather constant P_{81}/P_{83} ratios (Table 2). The largest variation in the Kr^{78}/Kr^{83} ratio is 15 percent (between rocks 10047 and 10057). Spallation Kr^{83} in rocks containing solar wind Kr were corrected for solar wind gases by using for the spallation component the lowest Kr^{86}/Kr^{83} ratio of rock-specimen 10017, 55, an interior sample, taking into account a contribution to Kr^{86} from spontaneous fission of U. The $Kr^{83}{}_{spall}/Kr^{81}$ ratio of an outside chip of rock 10017 was found to be 10 percent smaller than that of an inside sample, which may be attributed to a slightly higher Kr^{81} content. However, the relative errors in the Kr contents are about 6 percent.

Do the obtained Kr-Kr ages in fact give the actual time interval of exposure to cosmic rays? As has already been mentioned, there are obvious differences in the relative production rates of certain isotopes which cannot be explained by a varying chemical composition but only by differences in the composition and energy distribution of the interacting cosmic rays. Variations in the relative production of He^3 and Ne^{21} may in part be explained by differences in chemical composition or by possible diffusion losses. One is tempted to ascribe the observed variations in the relative production of the Kr isotopes to differences in the relative abundances of the target elements Sr, Y, and Zr. Large-scale variations in the relative production of the Xe isotopes, however, cannot be explained simply on the basis of chemical differences. Furthermore, the fact that specific relative production rates correlate with each other, such as the Kr^{78}/Kr^{83} and Xe^{126}/Xe^{131} ratios, leads us to conclude that the irradiation conditions of the four investigated rocks did differ from each other. The measured Xe^{131}/Xe^{126} ratios vary by almost a factor of 2 and are on the average also higher than the corresponding ratios found in meteorites. However, Pepin (*6*) found a Xe^{131}/Xe^{126} ratio of ≥ 5.3 in the Estherville meteorite, a value which is within the range covered by our four rocks and the soil sample. The evidence of such large relative Xe^{131} yields, which require a heavily moderated cosmic ray irradiation, suggests that special reactions may be partly responsible for the excess Xe^{131} production. Because of the high capture cross section, Gd is a sensitive indicator for thermal neutrons. We have measured the isotopic compositions of Gd in rock 10017 and in our soil sample. The depletion of Gd^{157} is between 0.1 and 0.4 percent for rock 10017, and for the soil sample we can give an upper limit of 0.2 percent. Because of background interferences in the Gd mass spectrum we can give only limits. This result shows that thermal neutron capture contributes less than 2 percent to the total Xe^{131} production. No neutron resonances are known for Ba^{130} and it seems unlikely that the neutron resonance integral will contribute much to the total cross section.

If the irradiation history of a rock is complex, if the rock has been partially and variably shielded from cosmic rays, then the reported radiation age represents only a lower limit for the actual time of irradiation. Our results indicate such complex histories at least for rocks 10017 and 10057 and for the soil sample.

K. MARTI
G. W. LUGMAIR
H. C. UREY

*Department of Chemistry,
University of California,
San Diego, La Jolla*

References and Notes

1. K. Marti, *Science* **166**, 1263 (1969).
2. F. Bühler, P. Eberhardt, J. Geiss, J. Meister, P. Signer, *ibid.* **166**, 1502 (1969).
3. K. Marti, *Earth Planet. Sci. Lett.* **2**, 193 (1967).
4. A. G. W. Cameron, *Icarus* **1**, 13 (1962).
5. K. Marti, *Phys. Rev. Lett.* **18**, 264 (1967).
6. R. O. Pepin, *J. Geophys. Res.* **71**, 2815 (1966).
7. L. H. Aller, *The Abundance of the Elements* (Interscience, New York, 1961).
8. H. E. Suess and H. C. Urey, *Rev. Mod. Phys.* **28**, 53 (1956).
9. A. G. W. Cameron, in *Handbook of Geophysics and Space Environments* (U.S. Air Force Cambridge Research Laboratories, Washington, D.C., 1965).
10. A. O. Nier, *Phys. Rev.* **79**, 450 (1950).
11. We thank K. R. Goldman and M. Meyers for valuable assistance. Supported by NASA contract NAS 9-8107.

5 January 1970

Isotopic Composition of Rare Gases in Lunar Samples

Abstract. *Data from total melt and step-by-step heating experiments on the Apollo 11 lunar samples suggest a close affinity between lunar and meteoritic rare gases. Trapped neon-20/neon-22 ratios range from 11.5 to approximately 15, resembling those for the gas-rich meteorites. Trapped krypton and xenon in the lunar fines and in the carbonaceous chondrites are similar except for an interesting underabundance of the heavy isotopes in both lunar gases which suggests that the fission component found in carbonaceous chondrites is depleted in lunar material. Spallation gases are in most cases quite close to meteoritic spallation gases in isotopic composition.*

Mass spectrometric analyses were carried out for all rare gas isotopes in six lunar crystalline rocks, a breccia, coarse fines sieved from the lunar soil, and the soil.

Gases in the crystalline rocks are in general dominated by radiogenic and spallogenic isotopes. The ^3He radiation ages, on the assumption of a ^3He production rate of 1×10^{-8} cm^3(STP) g^{-1} 10^6 $year^{-1}$, range from $\sim 30 \times 10^6$ (sample 10069,21) to 210×10^6 years (10071,20). U, Th-He, and K-Ar gas-retention ages, which are consistent with the values $\gtrsim 3.5 \times 10^9$ years reported in the preliminary analysis (*1*), as well as Ne, Ar, Kr, and Xe radiation ages, will be discussed in a later publication.

Neon isotopic compositions in the rocks and coarse fines are shown in Fig. 1. The pattern indicates a highly variable mixture of a single spallation composition, perhaps represented in virtually pure form in 10020,47[2], and a trapped neon component with $^{20}Ne/^{22}Ne = 12.7 \pm 0.4$. Neon in 10020,47[2] is essentially identical to that in the C3 and LL3 meteorites Felix and Chainpur, which terminate similar correlation lines for the carbonaceous chondrites (*2*). The striking variability in the proportion of trapped to spallation neon in repeat runs on certain samples may be a consequence of minute contamination by lunar fine material, despite care in handling and cleaning the rock chips. The large relative concentration of trapped Ne in the coarse fines (10085,5), which consisted of 1- to 2-mm fragments of fine- and coarse-grained crystalline rocks, probably derives from direct solar-wind irradiation of the fragment surfaces.

Light isotope compositions of Kr and Xe in four rocks and the coarse fines are shown in Figs. 2 and 3. The Kr points are colinear within the 1σ errors, and the correlation line passes through the composition of atmospheric Kr. The pattern indicates that these samples contain mixtures of an isotopically uniform spallation component and trapped Kr resembling terrestrial Kr. Scatter in the Xe points is somewhat larger; to a first approximation the trend is linear and the same conclusion holds. The trapped Xe component could be either atmospheric or carbonaceous chondrite Xe.

The spallation Kr spectrum, averaged over the four rocks shown in Fig. 2, is ^{78}Kr : ^{80}Kr : ^{82}Kr : ^{83}Kr : ^{84}Kr = 0.26 : 0.67 : $\equiv$ 1.00 : 1.36 : 0.59, and the spallation Xe spectrum, averaged over the three rocks 10020, 10045, and 10058, is ^{124}Xe : ^{126}Xe : ^{128}Xe : ^{129}Xe : ^{130}Xe : ^{131}Xe : ^{132}Xe : ^{134}Xe = 0.61 : $\equiv$ 1.00 : 1.50 : 1.78 : 0.84 : 3.98 : 0.8 : <0.1. The spectrums are derived assuming spallogenic ^{86}Kr and ^{136}Xe $\equiv$ 0. Both are similar to cosmic-ray spallation yields determined for two basaltic achondrites (*3, 4*). Xenon in the fourth rock (10072,21) differs from the achondritic spectrum in showing approximately a factor-2-larger relative production of ^{131}Xe and, to a lesser extent, ^{130}Xe. In this respect the spallation Xe in 10072,21 resembles that found in the silicate fraction of the Estherville mesosiderite, where ^{131}Xe : ^{126}Xe $\simeq$ 7.7 (*5*). These yields suggest a relatively soft irradiation spectrum.

Four bulk analyses—single-step melt-

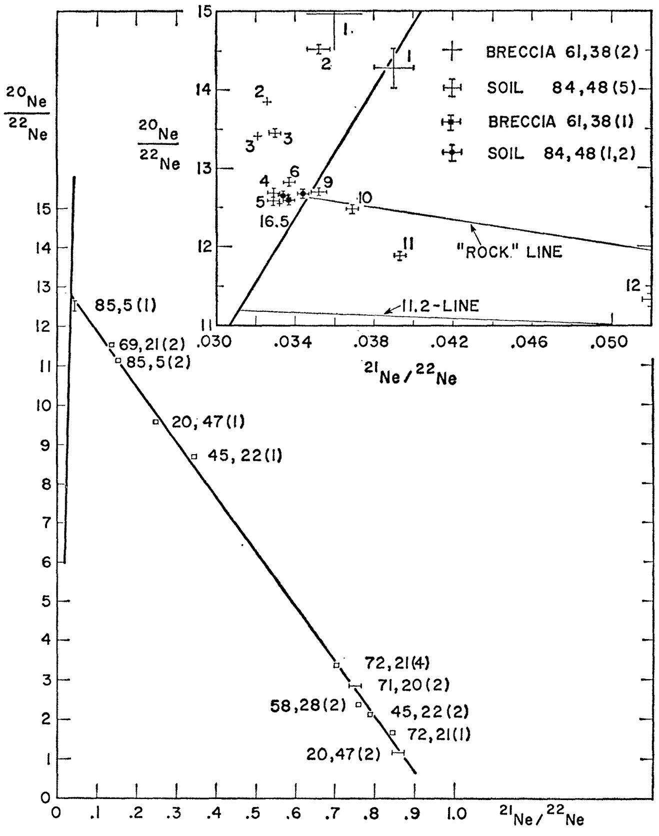

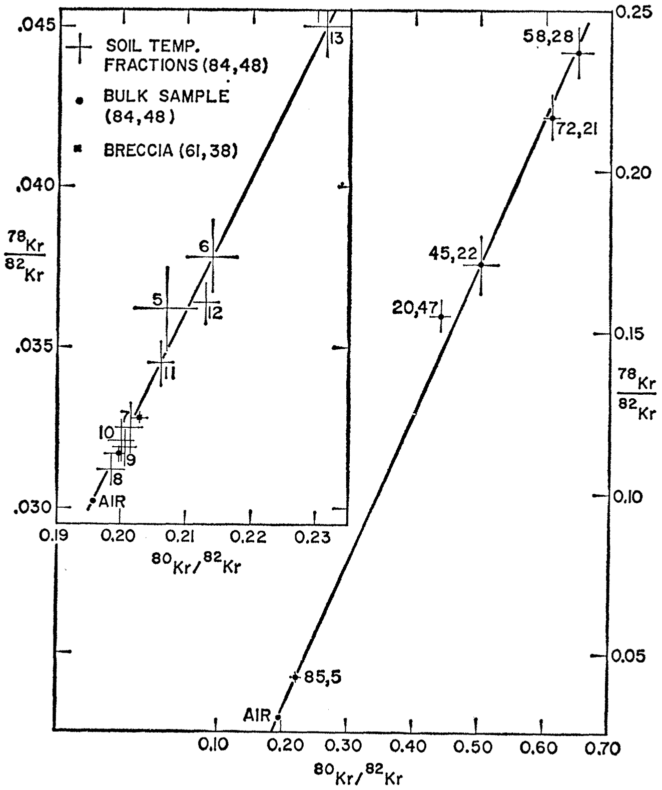

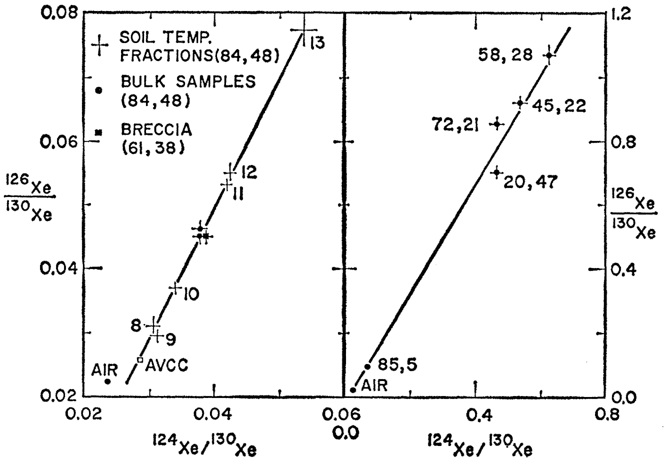

Fig. 1 (top left). Three-isotope correlations in Ne from lunar samples. Crystalline rocks are shown in the main diagram, with bulk and step-by-step heating data on fines and breccia in the insert. Errors are smaller than the plotted symbols except where indicated. Numbers in the insert are out-gassing temperatures in 100°C units; the 1300°C point for the soil lies well to the right of the diagram, slightly above the 11.2 line. Almost all Ne is released in the steps clustering around ^{20}Ne : ^{22}Ne = 12.6. The heavy diagonal and near-vertical lines are the meteoritic "trend line" (*6*). Fig. 2 (top right). Correlation diagram for the light Kr isotopes. Sample 85,5 in the main diagram is the coarse fines; others are crystalline rocks. Soil and breccia data are given in the insert. Fig. 3 (right). Correlation diagram for the light Xe isotopes, with rock and coarse fine data on the right and soil and breccia data on the left. On the right-hand scales the air and average-carbonaceous-chondrite-composition points are nearly indistinguishable, but on the left plot they are resolved and the correlation line clearly passes through the average carbonaceous chondrite composition.

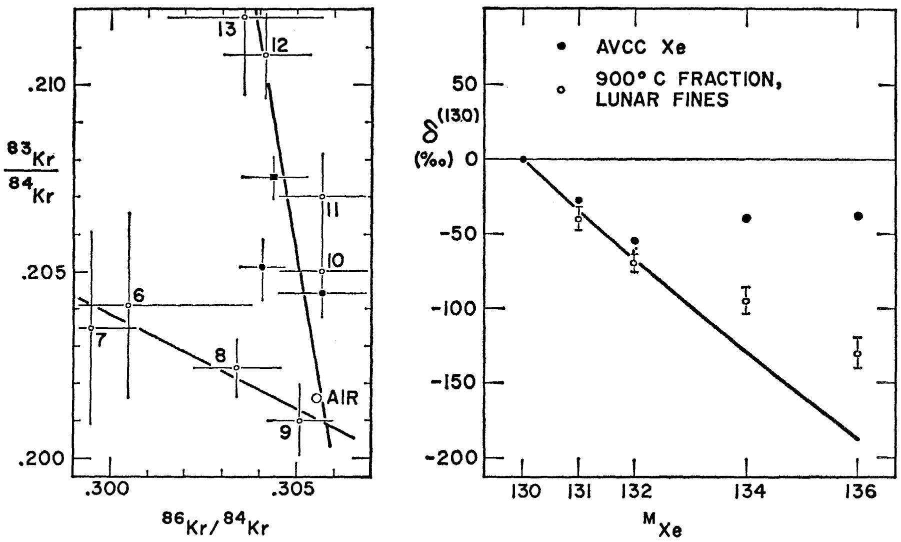

Fig. 4. Heavy Kr and Xe isotopes in the lunar fines and breccia. Filled points on the Kr correlation plot are bulk analyses of soil and breccia, open circles with numbers (100°C units) are step-by-step heating fractions. The lines appear to converge to the air point. All temperature fractions and bulk analyses of the fines and breccia show the general Xe depletion pattern displayed on the right-hand diagram by the 900°C fraction, but here the case is particularly clear because of minimum spallation interference at $^{130\text{-}134}$Xe.

ing extractions—were made on rare gases in the lunar fines and the breccia. In addition, step-by-step heating extractions and analysis of all rare gas isotopes in 13 100°C temperature steps were carried out on a sample of the fines.

Values of ^{4}He : ^{3}He = 2400, ^{4}He : ^{20}Ne≃100, ^{20}Ne : ^{22}Ne = 12.66, ^{36}Ar : ^{38}Ar = 5.38, and ^{40}Ar : ^{36}Ar = 1.07 are characteristic of bulk analyses of the soil, but He, Ne, and Ar isotopic ratios show considerable variation during step-by-step heating. The ^{4}He : ^{3}He ratio increases from ~1700 at 100°C to 3050 at 1000°C, then decreases to ~1100 at 1200°C. The ^{36}Ar : ^{38}Ar ratio falls monotonically from 5.77 at 200°C to 4.69 at 1300°C. In both cases the decrease at high temperature ($T \geq$ 1100°C) is due to a relatively large release of firmly sited spallation gases. The ^{40}Ar :^{36} Ar ratio is of particular interest, for the lunar fines contain about six times more ^{40}Ar than could have derived from *in situ* decay of ^{40}K over 4.5 × 10^{9} years, a difference which suggests that ^{40}Ar must be abundant in the trapped gases. A component which is probably radiogenic ^{40}Ar produced *in situ* outgases preferentially at low temperatures in the step-by-step heating: ^{40}Ar : ^{36}Ar = 14.4 in the 200°C fraction and falls to a minimum of 0.76 at 800°C, the point of maximum ^{36}Ar release and therefore the point at which the trapped gas composition is best represented.

Variations in Ne, Kr, and Xe isotopic compositions in the soil as functions of outgassing temperature are shown in Figs. 1–4. Neon, with very high ^{20}Ne : ^{22}Ne in the low-temperature fractions, is strikingly similar to Ne from step-by-step outgassing of the gas-rich achondrite Kapoeta, except that ^{21}Ne : ^{22}Ne ratios here are generally lower; points tend to lie to the left of the diagonal "trend-line" in the insert in Fig. 1 instead of moving along it as they typically do in meteorites *(6)*. It is clear that the principal Ne component in the lunar fines and breccias is one with ^{20}Ne : ^{22}Ne = 12.6 to 12.7, within error of the composition of neon-B (^{20}Ne : ^{22}Ne = 12.5±0.2), which dominates in the gas-rich meteorites. At high temperatures the neon composition trends toward spallation neon, with the trapped ^{20}Ne : ^{22}Ne ratio approaching 11.2, again a pattern characteristic of gas-rich meteorites (*6*). Except for the lower ^{21}Ne : ^{22}Ne, neon isotopic patterns in the lunar fines and the breccia and in the gas-rich meteorites are virtually identical.

The light-isotope variations in Kr and Xe in the fines, shown in Figs. 2 and 3, form linear arrays on the correlation diagrams. The patterns arise from variable mixing of isotopically uniform spallation and trapped gas components in the various temperature fractions. There is a suggestion in our results that the correlation lines for Kr and Xe in the soil and for Kr and Xe in the crystalline rocks (Figs. 2 and 3) may have slightly different slopes, and therefore that the isotopic compositions of the spallation components may be somewhat different in the two types of material. The apparent shift lies on the margin of experimental error. At the moment, to a first approximation, the soil and rock spallation components are similar.

The step-by-step heating correlation lines in Figs. 2 and 3 pass directly through the isotopic compositions of atmospheric Kr and average carbonaceous chondrite Xe, respectively. In all probability these are the compositions of trapped Kr and Xe in the lunar fines. It is clear that the trapped Xe is not terrestrial, since the air point lies well off the correlation in Fig. 3. If the composition of trapped Xe is assumed to be the average carbonaceous chondrite composition, a simple calculation shows that ~50 percent of the ^{126}Xe in the fines is spallogenic. On the basis of Ba and rare earth abundances in the fines (*7*) and Xe production rate equations developed by Marti *et al.* (*3*), the Xe radiation age of the lunar fines is ≃ 800 × 10^{6} years.

The possibility of atmospheric-type Kr as the trapped component in the fines is strengthened by the heavy isotope correlations shown in Fig. 4. There is evidence here for two spallation components, one appearing in the low-temperature fractions (600° to 900°C) and the other above 900°C. Both correlation lines pass near the composition of terrestrial Kr. The fractionated Kr composition reported to be present in carbonaceous chondrites (*8, 9*) lies well off this plot to the right and does not appear to be a constituent of lunar Kr.

The heavy Xe isotopes in the 900°C fraction of the fines are plotted in the right half of Fig. 4. Less than 0.5 percent of the ^{130}Xe in this fraction is spallogenic. The ordinate of the graph represents per mil deviations from atmospheric composition, normalized to ^{130}Xe. Current studies in this laboratory indicate that ~5 percent of atmospheric ^{136}Xe is fissiogenic. This component has been subtracted from the reference atmospheric Xe in Fig. 4. The heavy isotopes ^{134}Xe and ^{136}Xe are clearly depleted relative to the average carbonaceous chondrite Xe, a finding that suggests a depletion in the fission Xe component known to be present in the carbonaceous chondrites. However, some fission Xe is still present in lunar trapped Xe if our estimate of the composition of fission-free trapped Xe, shown by the heavy curve, is correct. This depletion of fission Xe, coupled with the absence of excess ^{86}Kr in lunar Kr and its definite presence in average carbonaceous chondrite Kr, suggests that excess ^{86}Kr and fission Xe concentrations may correlate, both resulting from the addition of a fissiogenic Kr-Xe component.

R. O. PEPIN
L. E. NYQUIST
DOUGLAS PHINNEY, DAVID C. BLACK
School of Physics and Astronomy,
University of Minnesota,
Minneapolis 55455

References and Notes

1. Lunar Sample Preliminary Examination Team, *Science* **165**, 1211 (1969).
2. R. O. Pepin, *Earth Planet. Sci. Letters* **2**, 13 (1967).
3. K. Marti, P. Eberhardt, J. Geiss, *Z. Naturforsch.* **21a**, 398 (1966).
4. C. M. Hohenberg, M. N. Munk, J. H. Reynolds, *J. Geophys. Res.* **72**, 3139 (1967).
5. R. O. Pepin, *ibid.* **71**, 2815 (1966).
6. D. C. Black and R. O. Pepin, *Earth Planet. Sci. Letters* **6**, 395 (1969).
7. V. R. Murthy, personal communication.
8. K. Marti, *Earth Planet. Sci. Letters* **3**, 243 (1967).
9. O. Eugster, P. Eberhrardt, J. Geiss, *ibid.* **3**, 249 (1967).
10. Supported by NASA contract NAS 9-8093, ONR contract Nonr-710(58), and NSF grant GA-905. A. O. C. Nier designed the 6-inch (15-cm) double-focusing mass spectrometer used for most of these analyses. We dedicate this paper to the late Rudolph B. Thorness for his 40 years of unparalleled contributions to mass spectrometry.

4 January 1970

Cosmic Ray Production of Rare Gas Radioactivities and Tritium in Lunar Material

Abstract. *The argon radioactivities ^{37}Ar and ^{39}Ar were obtained by vacuum melting from interior and exterior portions of rock 10057 and from a portion of the fines from the bulk sample container. The release of argon and tritium as a function of the temperature was followed for the fine material. A comparison is made of the activities observed in the lunar samples with those expected from the spallation of iron, titanium, and calcium. From these data and the ^{38}Ar content, the cosmic ray exposure age of rock 10057 is deduced as 110 × 10^6 years.*

A measurement of the stable and radioactive argon isotopes in lunar material can give valuable information on cosmic ray interactions on the lunar surface and can be used to deduce cosmic ray exposure ages of fragmented material resting on the lunar surface. Of particular interest are the stable isotopes ^{36}Ar and ^{38}Ar, and the radioactive isotopes ^{37}Ar (half-life, 35 days) and ^{39}Ar (half-life, 269 years). These isotopes are produced primarily by high-energy bombardment of the relatively abundant elements iron, titanium, and calcium. The primary goal of the investigation discussed here was to measure the ^{37}Ar and ^{39}Ar in surface rocks and in the fine material. The argon is evolved from the solid by vacuum melting and is counted in a small low-level gas proportional counter. By using pulse height analysis the Auger electron spectrum from the electron capture of ^{37}Ar can be easily distinguished from the beta spectrum of ^{39}Ar, and the two isotopes can be measured simultaneously. Since ^{37}Ar has a half-life of only 35 days, the measurements were made at the Lunar Receiving Laboratory during the biological quarantine.

The vacuum melting technique used to evolve and count the argon radioactivities also allows a search to be made for radioactive isotopes of the higher rare gases—namely ^{81}Kr, ^{85}Kr, ^{127}Xe, ^{133}Xe, and ^{222}Rn. The isotope ^{81}Kr (half-life, 2.1 × 10^5 years) has been observed in meteorites (*1*) and has been attributed to high-energy spallation of Sr, Y, and Zr. Radon-222 arises from the decay of ^{238}U, and a measurement of the ^{222}Rn content can be used as a sensitive measurement of the uranium concentration.

Of special interest is the tritium radioactivity in lunar materials that is also released by vacuum melting. This isotope is produced by high-energy cosmic ray bombardment. The rate of tritium production is an essential quantity needed to determine the tritium-^{3}He cosmic ray exposure age. Of far greater interest is the possibility that some of the solar flare particles are tritons. Fireman and his associates (*2*) observed tritium in the Discoverer 17 satellite and in a sounding rocket that was exposed to the solar flare of 12 November 1960. An analysis of their measurements indicates that the tritium-to-hydrogen ratio in this event was about 10^{-3} (*2*, *3*). A search for tritium in material exposed on the surface of the moon may afford a unique opportunity to remeasure the tritium content of solar flare particles.

Three separate samples of lunar material were studied; an internal (weight, 7.65 g) and an external (weight, 10.6 g) fragment of rock 10057, and a 10.6-g portion of the fine material (10002,6) from the bulk sample. Among the lunar rocks, the one designated 10057 has been classified type A; this includes the crystalline, fine-grained, vesicular rocks. The external rock fragment and the fine material were processed and measured at the Lunar Receiving Laboratory during the quarantine period, and therefore had to be heat-sterilized. The internal rock chip was measured after the quarantine period had ended, and was not sterilized. The sterilization was conducted in a stainless steel container at a temperature of 120°C for a period of 24 hours. A search was made for ^{37}Ar and ^{39}Ar released from the fine material during the heating and less than 0.6 disintegration min^{-1} kg^{-1} (dpm/kg) was found. The tritium released during the sterilization of the fine material was not determined because it was considered very likely that, if hydrogen were released, it would be absorbed into the stainless steel of the container.

Samples of lunar material in an alumina-lined molybdenum crucible were heated by a radio-frequency induction heater. The gases evolved were collected in a Toepler pump and placed in a tube containing hot vanadium metal. The vanadium at 850°C serves as a getter to remove chemically active constituents. The vanadium was then cooled to room temperature to absorb hydrogen as

Table 1. Volumes of rare gases and hydrogen from lunar material.

Sample	Extraction temperature (°C) and heating period	Rare gases (cm^3/g, STP)	Hydrogen (cm^3/g, STP)
Fines	Sterilization, 120, 24 hr	Not meas.	Not meas.
1000.2,6	120 to 600, 64 min	0.145	0.67
1000.2,6	600 to 900, 73 min	0.068	0.12
1000.2,6	900 to 1200, 92 min	0.003	0.04
1000.2,6	1200 to 1600, 68 min	<0.0005	<0.007
Total	120 to 1600	0.217	0.84
10057,3 (exterior)	120 to 1600	Not meas.	~ 0.1
10057,3 (interior)	120 to 1600	Not meas.	~ 0.16